We are IntechOpen, the world's leading publisher of Open Access books Built by scientists, for scientists

4,800
Open access books available

122,000
International authors and editors

135M
Downloads

Our authors are among the

154
Countries delivered to

TOP 1%
most cited scientists

12.2%
Contributors from top 500 universities

CLARIVATE ANALYTICS BOOK CITATION INDEX INDEXED

WEB OF SCIENCE™

Selection of our books indexed in the Book Citation Index in Web of Science™ Core Collection (BKCI)

Interested in publishing with us?
Contact book.department@intechopen.com

Numbers displayed above are based on latest data collected.
For more information visit www.intechopen.com

17

Bipedal Walking Pattern Design by Synchronizing the Motions in the Sagittal and Lateral Planes

Chi Zhu[1] and Atsuo Kawamura[2]
[1]*Maebashi Institute of Technology,* [2]*Yokohama National University*
Japan

1. Introduction

In these two decades, the technology of bipedal and humanoid robots has been made great progress. Up so far, many bipedal and humanoid robots are successfully developed (Hirai et al., 1998; Takanishi et al., 1985; Ogura et al., 2004; Kaneko et al., 2004; Nakasaka et al., 2004; Löffler et al., 2003; Lohmeier et al., 2004). In these robots, the gait planning and control for bipedal walking are based on ZMP concept (Vukobratovich et al., 1990; Goswami, 1999; Kakami, 2000). There are generally two methods for implementation of the dynamic and stable walking. The first one is based on a multiple rigid body robot model (Takanishi et al., 1985). This model is comparatively precise, but it requires a huge computation cost. The second one is simply based on the assumption that the whole robot mass is concentrated to robot's CoG (Center of Gravity). The typical approach is using a 3D inverted pendulum model (Kajita & Kobayashi, 1987; Kajita et al., 2002; 2003; Zhu et al., 2003, 2004), in which, the robot locomotion in the sagittal and lateral planes are supposed to be independent.

However, up to now, the bipedal walking nature and limitations of walking speed, stride, stride motion time, and so on, have not been completely understood. Partially this is because (1) few attentions are paid on the motion in double support phase and its effect to whole bipedal walking; (2) the investigation is not done intensively even for single support phase; for example, motion in sagittal plane are simply dealt with independent of the motion in lateral plane in most literatures on biped and humanoid robots. As revealed latter, in fact, such an approach is improper since the motions in the two planes are strongly coupled together. (3) ZMP is fixed to a point in robot sole for most of bipedal or humanoid robots.

This paper mainly discusses the above first two problems based on ZMP concept and an inverted pendulum model with the assumption that ZMP is fixed at the center of the robot sole in single support phase. To do this, the relation between the motions in the sagittal and lateral planes is investigated first. By dividing a whole bipedal walking cycle into a double support, a deceleration, and an acceleration phases, and synchronizing the motions in the sagittal and lateral planes, we point out that the motions in these two planes are strongly coupled together, in other words, the motion in the lateral plane greatly restricts the motion in the sagittal plane, vice versa. Then, the role of the double support phase in biped walking is discussed. By changing the start and finish points of the double support phases in the lateral plane, the walking parameters such as walking speed, walking period, phase stride

Source: Humanoid Robots: Human-like Machines, Book edited by: Matthias Hackel
ISBN 978-3-902613-07-3, pp. 642, Itech, Vienna, Austria, June 2007

and so forth, are consequently altered. With this, it comes a conclusion that a short double support phase is necessary in the viewpoint of both of a smooth and fast walking after a high enough instantaneous speed in the sagittal plane is obtained at the end of acceleration phase. Consequently, an approach for adjusting the instantaneous speed at the end of the acceleration phase is presented, and a biped walking planning procedure is proposed. Finally a numerical example is given out.

This paper is organized as follows. In Section 2, robot model, trajectories of the robot CoG and ZMP, and the general motion equations of the robot are described. In Section 3, a walking pattern with fixed ZMP is analyzed by being synchronized the motions in the two planes. In Section 4, the effects of the double support phase on bipedal walking are analyzed. Walking speed adjustment, walking planning, and an example are presented in Section 5, and the conclusion is given out in Section 6.

2. Robot Model and Bipedal Walking

2.1 Robot Model and Assumptions

In this study, a bipedal robot is modeled as a 3D inverted pendulum of which the mass of the robot is supposed to concentrate on the point C, the CoG of the robot, as shown in Fig.1. OXYZ is the world coordinate system, where X, Y axes are respectively the walking and swinging directions. XZ plane and YZ plane are respectively called the sagittal plane and lateral plane; and oxyz is the local system fixed to the center of the support sole of the robot. For simplicity, the following assumptions are made.

1. The height of the robot's CoG is a constant, i.e., $\ddot{z} = 0$.
2. The origin o of the local system oxyz is always set at the sole center of support foot.
3. The desired ZMP in single support phase (SSP) is also always set at the sole center of the support foot; hence, the desired ZMP in SSP is identical to o.
4. The equivalent foot length of two feet is b.
5. The robot moves with constant speed in the double support phase.

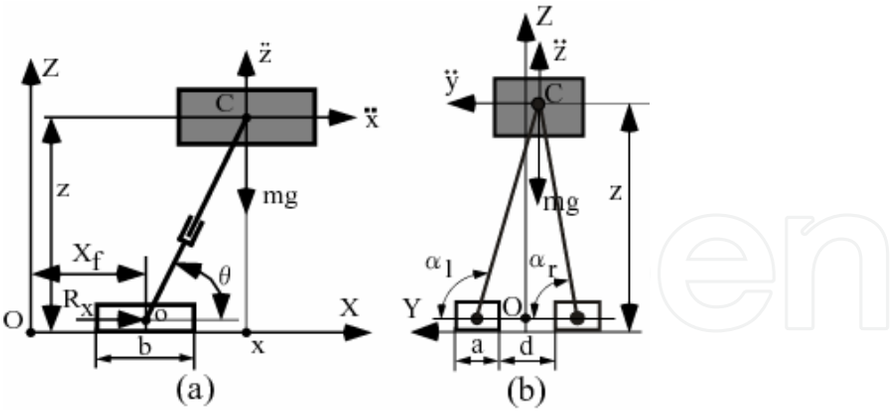

Figure 1. 3D inverted pendulum model of biped robot. (a) motion in sagittal plane. (b) motion in lateral plane

6. The robot just walks forward, i.e., the distance d0 in the lateral plane is a constant (Fig. 2).

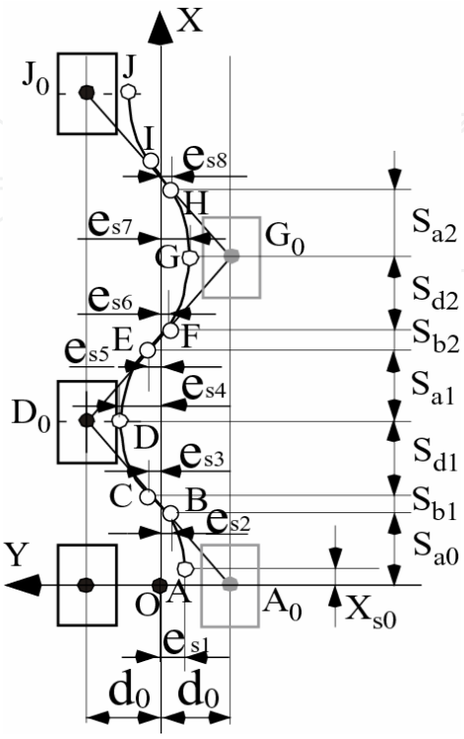

Figure 2. Trajectories of CoG and ZMP in bipedal walking

7. In single support phase, the CoG never passes over the X axis (the midline) of its two feet. This means that the single support phase ends and the double support phase starts before the CoG crosses the X axis.

Here, we make some explanations for the assumptions (2) and (3).

In theory, the origin o of the local system oxyz can be set at any place. Assumption (2) just brings a simple expression of the robot's motion equations (refer to Eqs. (5) and (6)). Hence, it leads great convenience for discussing the robot motion. Otherwise, if the origin o is not at the sole center of support foot, there would be respectively a constant offset in equations (5) and (6).

In SSP, ZMP (Zero moment point) is in fact a center of pressure of the support foot sole, or saying, the acting point of the resultant reaction force of the support floor. Therefore, ZMP is always within the inside of the sole of the support foot in SSP, even when the robot is falling down (at this moment, the ZMP is at one of the edges of the support foot). Consequently, the safest case is that the desired ZMP is at the sole center of the support foot in SSP.

Concretely, with the assumption of the desired ZMP at the sole center of the support foot, the motion equations of the CoG of the robot can be easily derived (as shown by Eqs. (5) and (6)), then this CoG motion is decomposed into each joint's motion (trajectory). The control system is just controlling each joint's motion as planned trajectory. In this way, the control system not only makes the biped robot stable walking, but also guarantees the real ZMP at the desired position (the sole center of the support foot). This approach is being used in most of biped humanoid robots, ex., (Kakami et al., 2000) and (Kajita et al., 2003).

When the real ZMP of the robot deviates from the desired ZMP, an additional on-line ZMP control scheme is necessary by modifying the CoG's motion (in fact, changing some or all joint's motion), for example, as did in (Zhu et al., 2004).
This paper just discusses the CoG's trajectory of the robot with the precondition of the desired ZMP at the sole center of the support foot in SSP, and doesn't consider the detail control problem.

2.2 Trajectories of Robot CoG and ZMP

The robot motion, in which its CoG trajectory is shown in Fig.2, is as follows. Before the robot starts to walk, its CoG is at the midpoint O of the two support feet. When the robot starts to walk, the CoG is first shifted from the point O to A. Here the distances between OA in X and Y direction are respectively X_{s0} and e_{s1}. From the point A, the left leg of the robot (here, assume the left leg of the robot first steps out) steps forward while the right leg supports the robot, and the robot moves forward along the curve AB. When the CoG moves to the point B, the left leg lands to the floor and the robot enters into the double support phase. When the CoG reaches to the point C, the right leg lifts off and the robot is in the single support phase again. During the left leg support phase, the CoG moves along the curve CDE. When the CoG reaches to E, the right leg lands to the floor and the robot is in the double support phase again. In this way, the swing leg and the support leg switches each other in turn at the points B, E, H, the robot moves forward in X direction (sagittal plane) while swings in Y direction (lateral plane). The positions of each point from A to H are shown in Fig.2.
As our assumptions indicate, the ZMP is fixed at the sole center of the support foot in the single support phase, such as points A_0, D_0, G_0, and J_0, and the ZMP moves from A_0 to D_0, from D_0 to G_0 in the double support phase as shown in Fig.2. In the local system *oxyz*, the ZMP can be expressed as

$$x_{ZMP} = x - \frac{\ddot{x}z}{g} \tag{1}$$

$$y_{ZMP} = y - \frac{\ddot{y}z}{g} \tag{2}$$

The above two equations can be rewritten as

$$\ddot{x} = \frac{g}{z}(x - x_{ZMP}) = g \cdot \cot\theta \tag{3}$$

$$\ddot{y} = \frac{g}{z}(y - y_{ZMP}) = g \cdot \cot\alpha \tag{4}$$

Eq.(3) shows that for the motion in the sagittal plane XZ, when the robot is forward leaning (the CoG of the robot is in front of the support foot, $x - x_{ZMP} \geq 0$, the robot has to accelerate forward. Contrarily, when the robot is backward leaning (the CoG is at the rear of the support foot, $x - x_{ZMP} \leq 0$), the robot should decelerate. Therefore, with the switching of the support leg and swinging leg in walking, the robot continually accelerates and decelerates.

In a single support phase, the general motion equations (the solutions of Eqs. (3) and (4) of the CoG of the robot in the two planes are respectively as follows,

$$x(t) = x_{ZMP} + c_1 \cdot e^{\omega t} + c_2 \cdot e^{-\omega t} \tag{5}$$

$$y(t) = y_{ZMP} + c_3 \cdot e^{\omega t} + c_4 \cdot e^{-\omega t} \tag{6}$$

where, x_{ZMP} and y_{ZMP} are respectively constants as our assumption; $\omega = \sqrt{g/z}$; c_1 to c_4 are coefficients determined by initial conditions.

3. Motions in Sagittal and Lateral Planes

In our previous work (Zhu et al., 2003, 2004), a bipedal walking is divided into initial acceleration, double support, deceleration and acceleration phases. Here the motion in each phase is investigated in more detail by combining and synchronizing the motion in the lateral plane. In this paper, the distances e_{sn} (n=0, 1, 2, ···) from the robot's CoG to X axis in Y direction (See Fig. 2) are supposed positive, i.e., $e_{sn} > 0$ (n=0, 1, 2, ···).

3.1 Initial acceleration phase AB

(Motion time: $0 \le t \le t_{a0}$, travelled distance in X and Y direction: $X_{s0} \le x(t) \le S_{a0}$, $-e_{s1} \le y(t) \le -e_{s2}$)

In this phase, the robot starts walking from the standstill and the robot has to accelerate. According to the motion equations (3) and (4), in order to guarantee the ZMP at the sole center of the support foot, the robot has to lean forward in the XZ (sagittal) plane and lean left in the YZ (lateral) plane, respectively. Thus, at the start point A, the offsets X_{s0} and e_{s1} respectively in X and Y axes are necessary as shown in Fig.2. (If $X_{s0} = 0$, then $x_{ZMP} = x$. It leads $\ddot{x} = 0$. This means the robot cannot move from the rest ($\dot{x} = 0$). If $e_{s1}=0$, then the robot will have to move to left and pass over the X axis. This violates the assumption (7)).

This condition implies that the projection of the CoG must be within the support polygon. This is (refer to Fig.1)

$$0 < X_{s0} \le \frac{b}{2} \tag{7}$$

With the initial conditions $x(0)=X_{s0}$, $\dot{x}(0) = 0$, $y(0)=-e_{s1}$, $\dot{y}(0)=0$, $x_{ZMP}=0$, and $y_{ZMP}=-d_0$, the coefficients of Eqs.(5) and (6) are respectively $c_1=c_2=X_{s0}/2$, and $c_3=c_4=(d_0 - e_{s1})/2$. Therefore the two motion equations are respectively

$$x(t) = \frac{1}{2} X_{s0}(e^{\omega t} + e^{-\omega t}) = X_{s0} \cdot \cosh(\omega t) \tag{8}$$

$$\begin{aligned} y(t) &= -d_0 + \frac{1}{2}(d_0 - e_{s1})(e^{\omega t} + e^{-\omega t}) \\ &= -d_0 + (d_0 - e_{s1})\cosh(\omega t) \end{aligned} \tag{9}$$

In the sagittal plane, the terminal conditions at the point B are

$$x(t_{xa0}) = \frac{1}{2} X_{s0}(e^{\omega t_{xa0}} + e^{-\omega t_{xa0}}) = S_{a0} \tag{10}$$

$$\dot{x}(t_{xa0}) = \frac{1}{2} \omega X_{s0}(e^{\omega t_{xa0}} - e^{-\omega t_{xa0}}) = V_{h0} \tag{11}$$

where, t_{xa0} and V_{h0} are respectively the motion time and terminal speed in the sagittal plane in this phase. From (10) and (11), t_{xa0} and V_{h0} can be respectively expressed as

$$e^{2\omega t_{xa0}} = \frac{\omega S_{a0} + V_{h0}}{\omega S_{a0} - V_{h0}} \tag{12}$$

$$V_{h0} = \omega \sqrt{S_{a0}^{\ 2} - X_{s0}^{\ 2}} \tag{13}$$

On the other hand, for the motion in the lateral plane, with the terminal conditions $y(t_{ya0})=-e_{s2}$ and $\dot{y}(t_{ya0}) = V_{ya0}$ (here, t_{ya0} and V_{ya0} are respectively the motion time and the terminal speed of the phase in the lateral plane). With the same way as done for the motion in the sagittal plane, t_{ya0} and V_{ya0} can be respectively expressed as

$$e^{2\omega t_{ya0}} = \frac{\omega(d_0 - e_{s2}) + V_{ya0}}{\omega(d_0 - e_{s2}) - V_{ya0}} \tag{14}$$

$$V_{ya0} = \omega \sqrt{(d_0 - e_{s2})^2 - (d_0 - e_{s1})^2} \tag{15}$$

Obviously, those two motions in the two planes should be synchronized, that is, there should be $t_{xa0}=t_{ya0}$. Thus, substituting Eqs. (13) and (15) into Eqs. (12) and (14) yields

$$\frac{X_{s0}}{S_{a0}} = \frac{d_0 - e_{s1}}{d_0 - e_{s2}} = \rho_{a0} < 1 \tag{16}$$

By substituting (16) into (12) or (14), we can get

$$e^{2\omega t_{a0}} = e^{2\omega t_{xa0}} = e^{2\omega t_{ya0}} = \left(\frac{1 + \sqrt{1 - \rho_{a0}^{\ 2}}}{\rho_{a0}} \right)^2 \tag{17}$$

Hence, the motion time in this phase is

$$t_{a0} = t_{xa0} = t_{ya0} = \frac{1}{\omega} \ln \frac{1}{\rho_{a0}} \left(1 + \sqrt{1 - \rho_{a0}^{\ 2}} \right) \tag{18}$$

By substituting (16) into (13) and (15), we can find the following relation

$$\frac{V_{ya0}}{V_{h0}} = \frac{d_0 - e_{s2}}{S_{a0}} \tag{19}$$

Moreover, from (16), there is

$$e_{s2}=\frac{1}{\rho_{a0}}e_{s1}+\left(1-\frac{1}{\rho_{a0}}\right)d_0=\frac{S_{a0}}{X_{s0}}e_{s1}+\left(1-\frac{S_{a0}}{X_{s0}}\right)d_0 \tag{20}$$

Since there should be $e_{s2}\geq 0$ as shown in Fig.2, there is

$$X_{s0}\leq\frac{d_0-e_{s1}}{d_0}S_{a0}=\left(1-\frac{e_{s1}}{d_0}\right)S_{a0} \tag{21}$$

If e_{s1} and e_{s2} are determined, then from (7) and (16), S_{a0} should be

$$S_{a0}<\frac{b}{2\rho_{a0}} \tag{22}$$

Eqs.(16), (20), and (21) show that the motions in the sagittal and lateral planes are tightly coupled together. The determination of the initial and terminal positions in one plane automatically and simultaneously decides the initial and terminal positions in another plane, therefore completely decides the motions in the two planes.
Eqs. (16) and (18) show that the motion time is independent of the moving distance, but determined by the ratio of the distance from the CoG to ZMP at the terminal time to the distance at the initial time in either of two planes. Eq. (19) shows that the ratio of the terminal velocities in the two planes is equal to the ratio of two distances from the CoG to ZMP at the terminal time in the two planes. Note that in this phase, an offset x_{s0} is necessary, otherwise the robot cannot start walking.

3.2 Double support phase BC

(Motion time: $0\leq t\leq t_{ds1}$, travelled distance in X and Y direction: $0\leq x(t)\leq S_{b1}$, $-e_{s2}\leq y(t)\leq e_{s3}$)

Once the CoG of the robot moves over the point B, the robot enters into the double support phase. We assumed that the robot moves forward with constant velocities V_{h0} and V_{ya0} respectively in X and Y directions. But its ZMP shifts from A_0 to D_0 (Fig. 2) in the double support phase. There are following initial and terminal conditions for ZMP's motion in this phase,

$$\dot{x}_{ZMP}(0)=0,\quad \dot{y}_{ZMP}(0)=0 \tag{23}$$

$$x_{ZMP}(0)=0,\quad y_{ZMP}(0)=-d_0 \tag{24}$$

$$\dot{x}_{ZMP}(t_{ds1})=0,\quad \dot{y}_{ZMP}(t_{ds1})=0 \tag{25}$$

$$x_{ZMP}(t_{ds1})=S_{a0}+S_{b1}+S_{d1},\quad y_{ZMP}(t_{ds1})=d_0 \tag{26}$$

Therefore, a third order polynomial function of time t is employed to represent ZMP's trajectory.

3.3 Deceleration phase CD

(Motion time: $0 \le t \le t_{d1}$, travelled distance in X and Y direction: $0 \le x(t) \le S_{d1}$, $e_{s3} \le y(t) \le e_{s4}$)

After the robot moves over the point C, its former support leg (here, is the right leg) will lift off and the robot is in the single support. Since the CoG of the robot is at the behind and right of its support foot, the robot must decelerate in both of two directions. This phase CD is called the *deceleration phase*.

With initial conditions x(0)=-S_{d1}, $\dot{x}(0) = V_{h0}$, y(0)=e_{s3}, $\dot{y}(0) = V_{ya0}$, and x_{ZMP}=0, y_{ZMP}=d_0, from Eqs.(5) and (6), the motion equations in the sagittal and lateral planes are respectively expressed as follows,

$$x(t) = \frac{V_{h0}}{\omega}\sinh(\omega t) - S_{d1}\cosh(\omega t) \tag{27}$$

$$y(t) = d_0 + \frac{V_{ya0}}{\omega}\sinh(\omega t) - (d_0 - e_{s3})\cosh(\omega t) \tag{28}$$

The terminal condition in the sagittal plane is x(t_{d1})=0, but $\dot{y}(t_{d1}) = 0$ for the lateral plane. In the same way as shown in subsection 3.1, the terminal speed V_{l1} (the lowest in this phase) in the sagittal plane is expressed as

$$V_{l1} = \sqrt{{V_{h0}}^2 - (\omega S_{d1})^2} \tag{29}$$

the swinging amplitude e_{s4} in this phase is

$$e_{s4} = d_0 - \sqrt{(d_0 - e_{s3})^2 - (V_{ya0}/\omega)^2} \tag{30}$$

Further, the motion times in the two planes are respectively as follows,

$$e^{2\omega t_{xd1}} = \frac{V_{h0} + \omega S_{d1}}{V_{h0} - \omega S_{d1}} \tag{31}$$

$$e^{2\omega t_{yd1}} = \frac{\omega(d_0 - e_{s3}) + V_{ya0}}{\omega(d_0 - e_{s3}) - V_{ya0}} \tag{32}$$

The above two motion times should be the same; therefore there exists the following condition,

$$\frac{V_{h0}}{\omega(d_0 - e_{s3})} = \frac{\omega S_{d1}}{V_{ya0}} \tag{33}$$

Consequently, by substituting (13), (15), and (16) into (33), the phase stride S_{d1} can be expressed as

$$S_{d1} = \frac{d_0 - e_{s2}}{d_0 - e_{s3}} S_{a0}(1 - {\rho_{a0}}^2) \tag{34}$$

Meanwhile, to guarantee the robot continually moving forward, the terminal speed should be $V_{l1}>0$, that is

$$\omega S_{d1} < V_{h0} \tag{35}$$

With (13) and (14)), the condition (35) implies that

$$0 < e_{s3} < d_0 - (d_0 - e_{s2})\sqrt{1-\rho_{a0}{}^2} \tag{36}$$

Further, by substituting Eqs. (29) and (30)) into Eqs. (31)) and (32), we can get

$$e^{2\omega t_{xd1}} = \frac{1+\sqrt{1-\left(\frac{V_{l1}}{V_{h0}}\right)^2}}{1-\sqrt{1-\left(\frac{V_{l1}}{V_{h0}}\right)^2}} = \frac{\left(1+\sqrt{1-\left(\frac{V_{l1}}{V_{h0}}\right)^2}\right)^2}{\left(\frac{V_{l1}}{V_{h0}}\right)^2} \tag{37}$$

$$e^{2\omega t_{yd1}} = \frac{1+\sqrt{1-\left(\frac{d_0-e_{s4}}{d_0-e_{s3}}\right)^2}}{1-\sqrt{1-\left(\frac{d_0-e_{s4}}{d_0-e_{s3}}\right)^2}} = \frac{\left(1+\sqrt{1-\left(\frac{d_0-e_{s4}}{d_0-e_{s3}}\right)^2}\right)^2}{\left(\frac{d_0-e_{s4}}{d_0-e_{s3}}\right)^2} \tag{38}$$

Thus, there are the following relations,

$$\frac{V_{l1}}{V_{h0}} = \frac{d_0-e_{s4}}{d_0-e_{s3}} = \rho_{d1} < 1 \tag{39}$$

$$e_{s4} = (1-\rho_{d1})d_0 + \rho_{d1}e_{s3} \tag{40}$$

and the motion time t_{d1} is

$$t_{d1}=t_{xd1}=t_{yd1}=\frac{1}{\omega}\ln\frac{1}{\rho_{d1}}\left(1+\sqrt{1-\rho_{d1}{}^2}\right) \tag{41}$$

Note that when $e_{s3}=e_{s2}$, there is a following relations,

$$e_{s4} = e_{s1} \quad \text{and} \quad t_{d1} = t_{a0} \quad (\text{as } e_{s3} = e_{s2}) \tag{42}$$

3.4 Acceleration phase DE

(Motion time: $0 \le t \le t_{a1}$, travelled distance in X and Y direction: $0 \le x(t) \le S_{a1}$, $e_{s5} \le y(t) \le e_{s4}$)

In the sagittal plane, once passing over the point D, the CoG of the robot will be in front of its support foot. Thus, the robot must accelerate. On the other hand, the robot reaches its

swinging peak at D with zero speed, and its CoG is in the right of its support foot. Therefore, the robot will accelerate in the lateral plane, too. This phase is called the *acceleration phase*.

With the initial conditions x(0)=0, $\dot{x}(0) = V_{l1}$, y(0)=e_{s4}, $\dot{y}(0) = 0$, and x_{ZMP}=0, y_{ZMP}=d_0, from Eqs.(5) and (6), the motion equations in the sagittal and lateral planes are respectively,

$$x(t) = \frac{V_{l1}}{\omega}\sinh(\omega t) \tag{43}$$

$$y(t) = d_0 - (d_0 - e_{s4})\cosh(\omega t) \tag{44}$$

The terminal conditions are x(t_{a1})=S_{a1}, y(t_{a1})=e_{s5}. In the same way as shown in subsection 3.1, the terminal speed V_{h1} and V_{ya1} in the two planes are respectively

$$V_{h1} = \sqrt{{V_{l1}}^2 + (\omega S_{a1})^2} \tag{45}$$

$$V_{ya1} = \omega\sqrt{(d_0 - e_{s5})^2 - (d_0 - e_{s4})^2} \tag{46}$$

These two velocities are the highest in this phase. Further, the motion time in the two planes can be respectively expressed as follows,

$$e^{2\omega t_{xa1}} = \frac{V_{h1} + \omega S_{a1}}{V_{h1} - \omega S_{a1}} \tag{47}$$

$$e^{2\omega t_{ya1}} = \frac{\omega(d_0 - e_{s5}) + V_{ya1}}{\omega(d_0 - e_{s5}) - V_{ya1}} \tag{48}$$

With the condition t_{xa1}=t_{ya1}, by rewriting (45) to express ωS_{a1} in terms of V_{h1} and V_{l1}, and by substituting (46) into (48), then we can get the following condition,

$$\frac{V_{h1}}{V_{l1}} = \frac{d_0 - e_{s5}}{d_0 - e_{s4}} = \rho_{a1} \tag{49}$$

From (49), e_{s5} can be expressed as

$$e_{s5} = (1 - \rho_{a1})d_0 + \rho_{a1}e_{s4} \tag{50}$$

Further, from Eqs. (29), (39), (45), and (49), the following three relations can be derived out,

$$S_{a1} = \sqrt{\frac{(d_0 - e_{s5})^2 - (d_0 - e_{s4})^2}{(d_0 - e_{s3})^2 - (d_0 - e_{s4})^2}} \cdot S_{d1} \tag{51}$$

$${V_{h1}}^2 - {V_{h0}}^2 = \omega^2\left({S_{a1}}^2 - {S_{d1}}^2\right) \tag{52}$$

$$\frac{V_{h1}}{V_{h0}} = \frac{d_0 - e_{s5}}{d_0 - e_{s3}} \tag{53}$$

These three equations are used to adjust the terminal speed V_{h1} of the acceleration phases. It will be discussed in Section 5. Note that e_{s4} is a function of e_{s3} and determined by eq.(30).
According to our assumptions, there is $e_{s5}>0$, hence from (45) and (49), the phase stride S_{a1} should be determined by

$$S_{a1} < \frac{V_{l1}}{\omega}\sqrt{\left(\frac{d_0}{d_0 - e_{s4}}\right)^2 - 1} \tag{54}$$

Similar to be done in subsection 3.1, the motion time t_{a1} in this phase is

$$t_{a1}=t_{xa1}=t_{ya1}=\frac{1}{\omega}\ln\left(\rho_{a1}+\sqrt{\rho_{a1}^{\ 2}-1}\right) \tag{55}$$

Note that BCDE is a whole walking cycle which consists of a double support, a deceleration, and a acceleration phases. After the acceleration phase, the robot will enter into the double support phase and start a new walking cycle again. Similar to the deceleration phase CD, for the second deceleration phase FG, we can get

$$S_{d2} = \frac{d_0 - e_{s4}}{d_0 - e_{s6}}\rho_{a1}S_{a1} = \frac{d_0 - e_{s5}}{d_0 - e_{s6}}S_{a1} \tag{56}$$

and since $V_{l2} = \sqrt{V_{h1}^{\ 2} - (\omega S_{d2})^2} > 0$, there is

$$\begin{aligned} 0 < e_{s6} < e_{s6\max} &= d_0 - \sqrt{1 - \frac{1}{\rho_{a1}^{\ 2}}}\cdot(d_0 - e_{s5}) \\ &= d_0 - \sqrt{(d_0 - e_{s5})^2 - (d_0 - e_{s4})^2} \end{aligned} \tag{57}$$

From the second deceleration phase, the motion is repetitive and the equations are also the same.

4. Double Support Phase and Bipedal Walking

The discussion in Section 3 shows that the motions in the sagittal and lateral planes are strongly coupled together. It also indicates that the initial and terminal points of the double support phases, such as points B, C, E, F, H, I in Fig. 2, greatly affects the robot motion. This section further illustrates the effects of the double support phase to the bipedal walking.
To let the discussion be more general, we discuss the motion in the second walking cycle EFGH in Fig. 2, where, EF is the double support phase, FG and GH are respectively the deceleration and acceleration phases. We assume that when the robot travels to the point E,

the parameters before E such as e_{s4}, e_{s3}, S_{d1}, and etc, are determined and known. Here, the parameters used are z=0.50 [m], e_{s1}=0.07 [m], $e_{s2}=e_{s3}=e_{s5}$=0.02 [m].

4.1 Double support phase and deceleration phase

As discussed in Section 3, e_{s5}, or saying, the position of the point E, determines the velocities at the point E that is equal to the velocities at the point F as we assumed. Meanwhile, e_{s6}, the terminal position of the point F of the double support phase EF, affects the motion in phase FG, too. Therefore, both e_{s5} and e_{s6} determine the motion in deceleration phase FG. Note that the selection of e_{s6} should satisfy the condition of ineq.(57), in which, e_{s6max} is the function of e_{s5}, i.e., $e_{s6max}=e_{s6max}$ (e_{s5}).

With the variations e_{s5} and e_{s6}, in the phase FG, the motion parameters such as the swinging amplitude e_{s7}, motion time t_{d2}, phase stride S_{d2}, the speed V_{l2} at point G (the lowest one in a whole walking cycle), and the average speed Av_{l2}, will correspondingly change. Their relations with e_{s5} and e_{s6} are respectively shown from Fig. 3 to Fig. 7. In these figures, there are 7 curves corresponding to e_{s5}=0 to e_{s5}=0.07[m] of which the interval of e_{s5} is Δe_{s5}=0.01 [m], and all of these 7 curves start from e_{s6}=0 and end at $e_{s6}=e_{s6max}$ (e_{s5}).

Fig. 3 to Fig. 7 respectively show that for

- *e_{s5} fixed but e_{s6} variable case*
  e_{s7}, t_{d2}, and S_{d2} increase, but V_{l2} and Av_{l2} decrease with e_{s6}. Note that (1) a fixed e_{s5} implies that phase stride S_{a1}, the velocities of V_{h1} and V_{ya1} are determined; (2) when $e_{s6}=e_{s5}$, there are $e_{s7}=e_{s4}$, $t_{d2}=t_{a1}$, $S_{d2}=S_{a1}$, and $V_{l2}=V_{l1}$; (3) if $e_{s6}=e_{s6max}$ (e_{s5}), then $e_{s7}=d_0$, $t_{d2} \to \infty$, $S_{d2}=S_{d2max}=V_{h1}/\omega$, V_{l2}=0, and Av_{l2}=0 since the robot will stop at the point G in this extreme case.
- *e_{s6} fixed but e_{s5} variable case*
  e_{s7}, t_{d2}, and S_{d2} monotonously decrease with e_{s5}, but V_{l2} and Av_{l2} have not such monotonicity (e_{s5} and e_{s6} should be subject to the condition of ineq.(57). Note that (1) the increase of e_{s5} means the decrease of S_{a1}, V_{h1}, and V_{ya1}; (2) when $e_{s5}=e_{s5max}=e_{s4}$ (=0.07[m], there are $e_{s7}=e_{s6}$, $S_{d2}=S_{a1}$=0, $t_{d2}=t_{a1}$=0, and $V_{l2}=V_{l1}$; in other words, the acceleration phase DE and the deceleration phase FG will disappear; (3) when $e_{s5}=e_{s6}$=0, there is $V_{l2}=V_{l1}$; (4) for a given e_{s6}, there exists a V_{l2max} occuring at a e_{s5}; for example, when e_{s6}=0, V_{l2max}=1.00[m/s]; as e_{s5}=0.0248[m]; (5) similarly, for a given e_{s6}, there exists a Av_{l2max} at a e_{s5}; for instance, when e_{s6}=0, Av_{l2max}=1.16[m/s]; as e_{s5}=0.0167[m] as shown in Fig. 7.

The above phenomena can be explained by the equations discussed in above section just by substituting e_{s4}, e_{s5}, S_{d1}, S_{a1} respectively with e_{s7}, e_{s8}, S_{d2}, S_{a2}, and so forth.

A big V_{l2} (here, V_{h1} is fixed with a fixed e_{s5}) implies a small speed fluctuation (V_{h1} - V_{l2}) and a smooth bipedal walking; meanwhile a big Av_{l2} means the robot walks fast. Therefore, Fig. 6 and Fig. 7 show that small e_{s5} and e_{s6} should be selected in the view of both of smooth walking and fast walking.

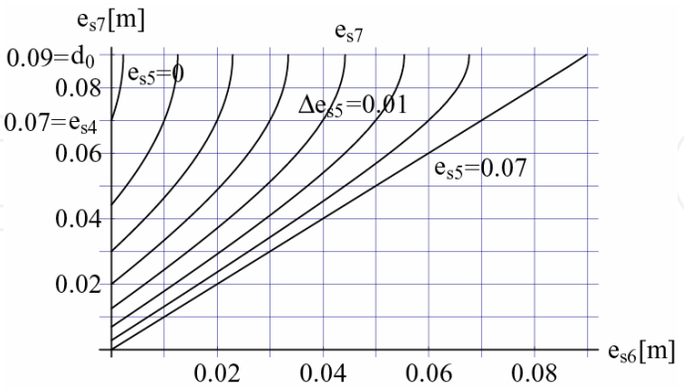

Figure 3. Variation of swinging amplitude e_{s7} with e_{s5} and e_{s6}

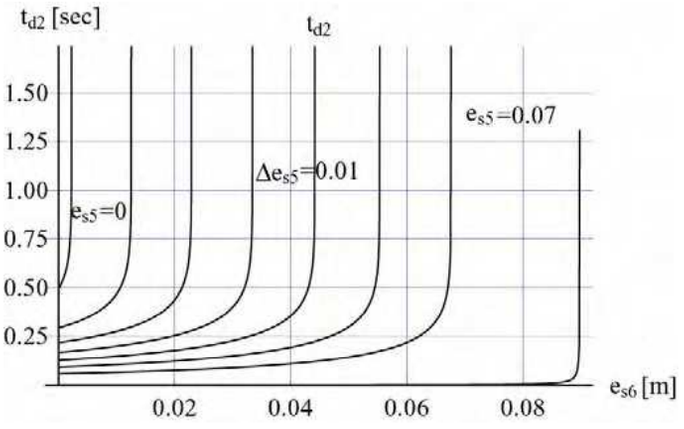

Figure 4. Variation of t_{d2} with e_{s5} and e_{s6}

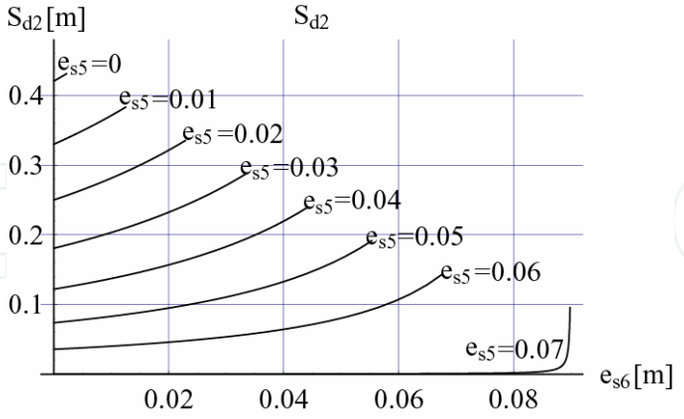

Figure 5. Variation of S_{d2} with e_{s5} and e_{s6}

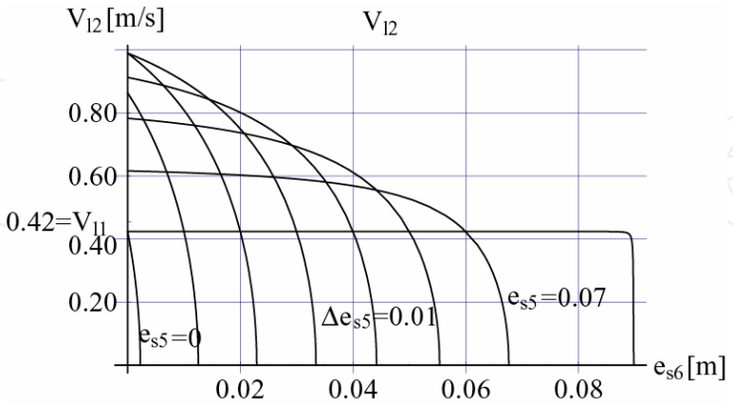

Figure 6. Variation of V_{l2} with e_{s5} and e_{s6}

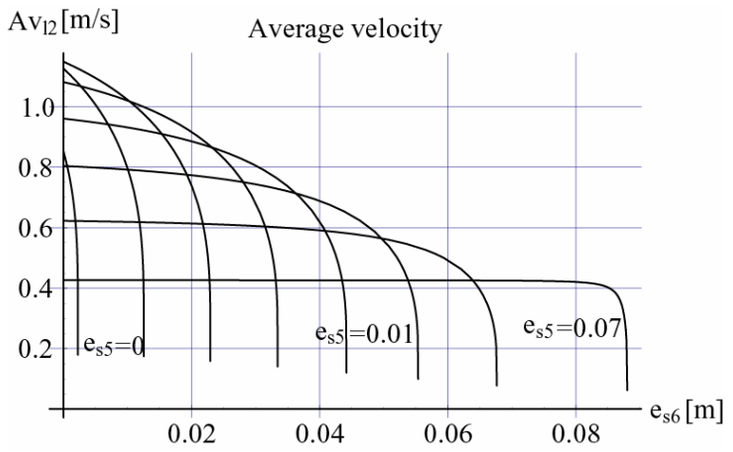

Figure 7. Variation of average speed Av_{l2} with e_{s5} and e_{s6}

4.2 Double support phase and acceleration phase

Here, we mainly discuss the effects of e_{s6} and e_{s8} to the motion in acceleration phase GH, because these two parameters determine the motion of the acceleration phase GH. For simplicity, here e_{s5} is set to be equal to e_{s3}, i.e., $e_{s5}=e_{s3}=0.02$[m] (refer to Table. 1. Therefore, the variable ranges of e_{s6} and e_{s8} are respectively $0<e_{s6}<e_{s6max}$ (e_{s5}) (=0.0229[m] and $0<e_{s8}< e_{s7}$ (e_{s6}). As described in subsection 4.1, here e_{s7} is the function of e_{s6}, and e_{s7} (e_{s6max})= d_0. Similarly to subsection 4.1, with the variations of e_{s6} and e_{s8}, the motion parameters, such as the phase stride S_{a2}, motion time t_{a2}, speed V_{h2} and V_{ya2} at point H, and the average speed Av_{a2} in phase GH, will change. Their change figures are respectively illustrated from Fig. 8 to Fig. 12. In these figures, there are 8 curves corresponding to e_{s6}=0 to e_{s6}=0.021[m] of which the interval of e_{s6} is Δe_{s5}=0.03[m], and all of these 8 curves start from e_{s8}=0 and end at $e_{s8max}=e_{s7}$ (e_{s6}), where e_{s7} (e_{s6}) means e_{s7} is the function of e_{s6}.

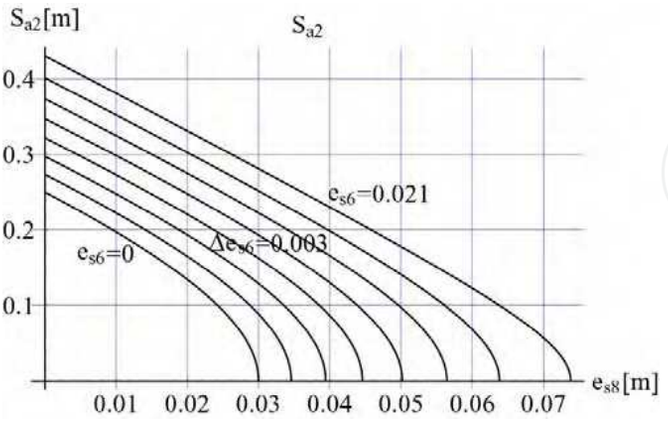

Figure 8. Variation of S_{a2} with e_{s6} and e_{s8}

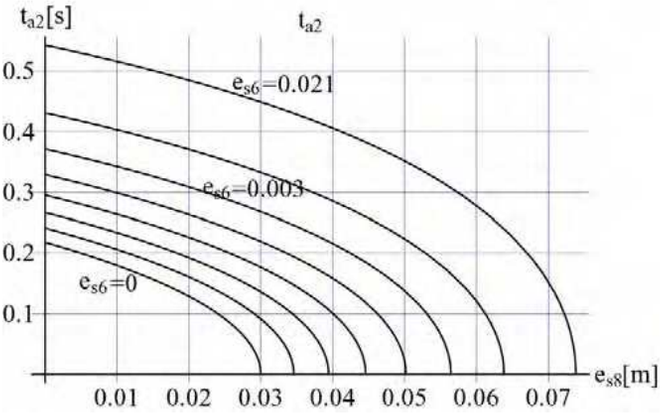

Figure 9. Variation of t_{a2} with e_{s6} and e_{s8}

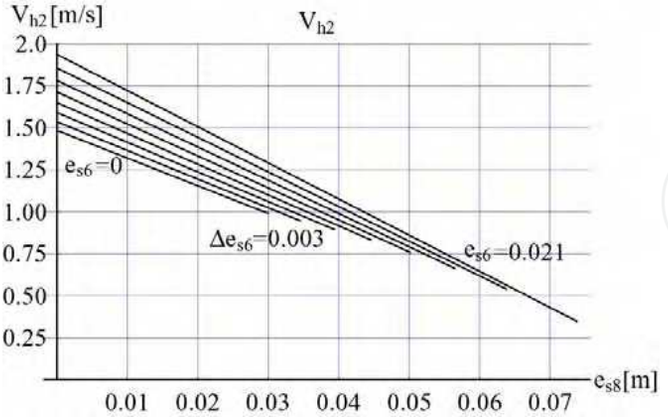

Figure 10. Variation of V_{h2} with e_{s6} and e_{s8}

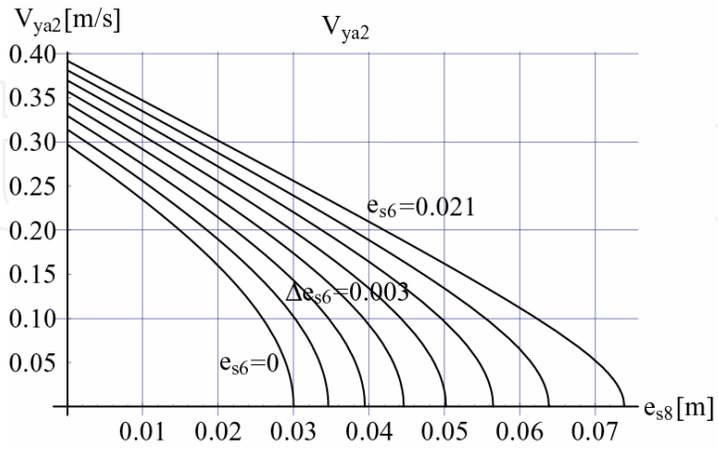

Figure 11. Variation of V_{ya2} with e_{s6} and e_{s8}

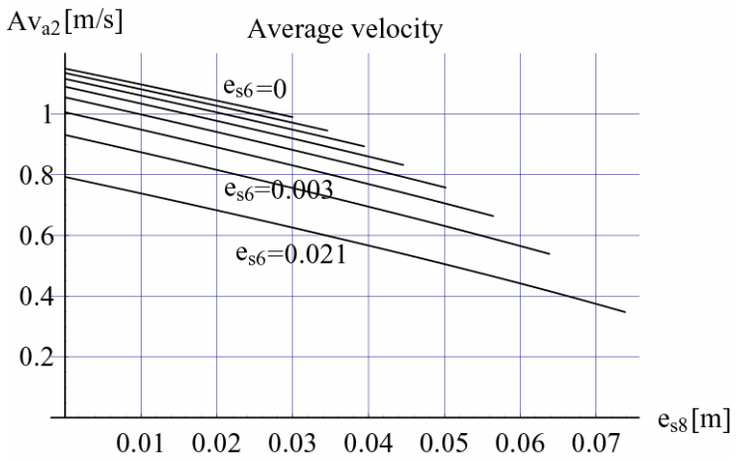

Figure 12. Variation of V_{ya2} with e_{s6} and e_{s8}

Fig. 8 to 12 show that

- *e_{s6} fixed but e_{s8} variable case*
  All of S_{a2}, t_{a2}, V_{ya2}, V_{h2}, and Av_{a2} decrease with e_{s8}. For a fixed e_{s6}, the position of point G (e_{s7}, S_{d2}) and the velocity at G are determined. Thus, the above phenomenon is very straightforward. Note that when $e_{s8}=e_{s7}(e_{s6})$, then there are $S_{a2}=0$, $t_{a2}=0$, $V_{ya2}=0$, $V_{h2}=V_{l2}$, i.e., the double support phase HI will be longest and the acceleration phase GH will disappear.
- *e_{s8} fixed but es6 variable case*
  S_{a2}, t_{a2}, V_{ya2}, and V_{h2} increase, but Av_{a2} decrease with e_{s6}. Note that as aforementioned, when $e_{s6}=e_{s6max}(e_{s5})$, the robot will stop at the point G and cannot enter acceleration phase. Here, this extreme case is omitted.

A high V_{h2} means a high terminal speed, while a low V_{h2} implies a smooth walking. Meanwhile a big Av_{a2} means a fast walking. Thus, Fig. 10 and 12 show that both of small e_{s6} and e_{s8} are favorite in the view of both of smooth walking and fast walking.

5. Motion Planning and Numerical Example

5.1 Speed Adjustment during Walking

In section 4, we repeatedly point out that a short double support phase (saying, small e_{s5}, e_{s6}, e_{s7}, and etc.) is necessary for a smooth and fast walking. Of course, there is a premise for fast walking, that is, the robot should possess a high enough speed in the sagittal plane before entering a new double support phase. If not, because a short double support phase results in short phase stride and cannot change the robot velocities greatly, therefore the short double support phase cannot produce a fast walking (in this sense, the ability of speed adjustment of a short double support phase is weak). Consequently, we are confronted with a problem: how to get a high speed before entering a new walking cycle.

(The V_{h1} below means the terminal speed at the end of an acceleration phase, while V_{h0} implies the terminal speed at the end of the previous acceleration phase.)

With Eqs. (51) to (53), it is easily concluded that

1. $V_{h1}=V_{h0}$ requires $S_{a1}=S_{d1}$ or $e_{s5}=e_{s3}$. The walking cycle is called *isometric speed cycle*.
2. $V_{h1}>V_{h0}$ implies $S_{a1}>S_{d1}$ or $e_{s5}<e_{s3}$. The walking cycle is *accelerated*. In other words, if the start point (ex., point E) of a double support phase is closer to the midline (X axis) of two feet than the finish point (ex., point C) of the previous double support phase, the robot will be accelerated.
3. Contrarily, $V_{h1}<V_{h0}$ means $S_{a1}<S_{d1}$ or $e_{s5}<e_{s3}$. The walking cycle is *decelerated*.

Note that the above three conditions also imply that if the landing point D_0 is just at the midpoint of CE (Fig. 2), then the robot will just make an isometric speed walking; if the landing point D_0 is at the rear of the midpoint of CE, the robot will accelerate; contrarily, the robot will decelerate if the point D_0 is in front of the midpoint of CE. Thus, by adjusting the phase stride S_a and S_d, or the positions e_{s2}, e_{s3}, e_{s5}, e_{s6}, and e_{s8} of which the start and finish points of double support phases, the walking speed can be changed.

5.2 Motion Planning

To generalize the above discussions, an example of bipedal walking planning for ZMP fixed case is given out, in which, there are two walking cycles BCDE and EFGH. The first one, BCDE, makes an isometric speed walking and the second one, EFGH, is acceleration walking. Here, parameters z or ω, and d_0 are known.

Initial acceleration phase:

1. Determine e_{s1}, e_{s2} and calculate ρ_{a0}.
2. Determine S_{a0} with condition (22).
3. Calculate X_{s0}, V_{ya0}, V_{h0}, and t_{a0}.

Generally, a big e_{s1} results in a big S_{a0} and a high V_{h0}.

Double support phase:

1. Determine e_{s3} or e_{s6}.
2. Calculate motion time t_{b1} and t_{b2}.
3. Calculate S_{d1} or S_{d2} with (34) or (56).
4. Determine moving distances of CoG in two directions and determine ZMP function in sagittal plane.

Deceleration phase:
1. Calculate V_{l1} and ρ_{d1} or V_{l2} and ρ_{d2}.
2. Calculate e_{s4} or e_{s7}, and t_{d1}, t_{d2}.

Acceleration phase:
1. Determine e_{s5} or e_{s8}.
2. Calculate S_{a1} or S_{a2}.
3. Calculate ρ_{a1}, V_{ya1}, V_{h1}, t_{a1}, or ρ_{a2}, V_{ya2}, V_{h2}, and, t_{a2}.

5.3 Numerical Example

Parameters used for motion planning are as follows: z=0.50[m], b=0.22[m]. Here, for the first walking cycle BCDE, $e_{s5}=e_{s3}=e_{s2}$, thus this cycle is an isometric speed one. For the second one EFGH, $e_{s8}<e_{s6}<e_{s5}$, it means this cycle is accelerated. In this example, the robot is simply accelerated in the initial acceleration phase AB, since the speed V_{h0} is high enough because of a big S_{a0}. Further, the robot is slightly accelerated in the second walking cycle.

The trajectories and velocities in X and Y directions of the robot's CoG, and ZMP's trajectories in X and Y directions are respectively shown in Fig. 13 to 18. The motion parameters shown in Fig. 13 to Fig. 18 are listed in Table 1. The average speed of the first cycle is about 3.05[km/h], while the one of the second cycle is about 4.04[km/h]. Note that in the second walking cycle, the swinging amplitude e_{s7} gets more narrow, the motion time t_{d2} and t_{a2} are shorter, but the phase strides S_{d2} and S_{a2} only get slightly shorter. Such a walking pattern is very similar to what a walker does in walking race, where the walker's swinging amplitude is small and the walking period is short, but his step length is not changed so much. Resultantly his walking speed is high. (In our example, the speed of the robot is about 4[km/h], but generally a walker's speed in walking race is over 10 [km/h], since the ZMP is variable from the heel to the toe in walking. The bipedal walking based on variable ZMP is beyond the scope of this paper.)

6. Conclusion

In this paper, a new design approach of bipedal walking pattern based on the synchronization of the motions in the sagittal and lateral planes are presented. With the discussion on the motions in these two planes, the fact is clarified that the motions in the sagittal and lateral planes are tightly coupled together. The motion parameters in the sagittal plane such as walking speed, walking time, and phase stride can be easily adjusted by altering the start and finish points of the double support phase in the lateral plane. Therefore, an approach for adjusting the walking speed by controlling the double support phase is naturally developed. Moreover, it is pointed out that a smooth and fast walking can be obtained by shortening the double support phase after a high speed is reached at the end of acceleration phase. Such a walking pattern is very similar to a walker's patter in walking race. The motion planning is also presented and a numerical example is given out. It is expected to apply this theory to a real bipedal robot and extend it to the jumping and running robot.

(This paper is originally published in IEEJ Trans. IA, Vol. 126, No. 8, pp. 1069-1078, 2006)

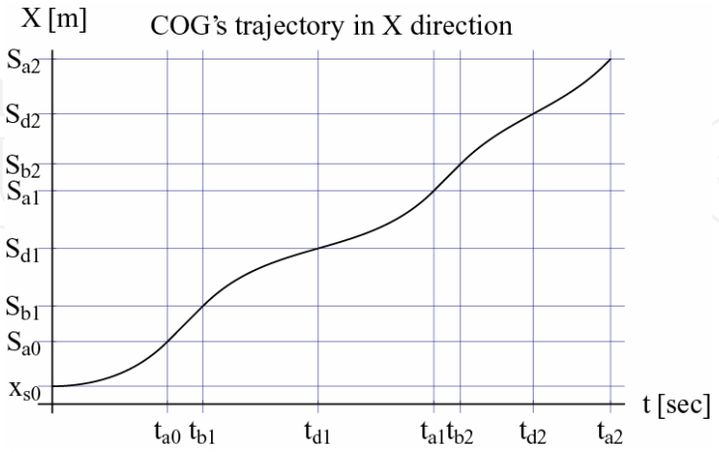

Figure 13. CoG's trajectory in X direction

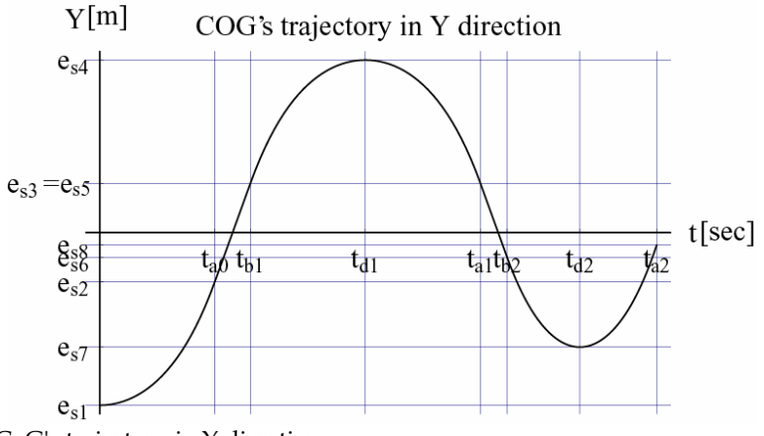

Figure 14. CoG's trajectory in Y direction

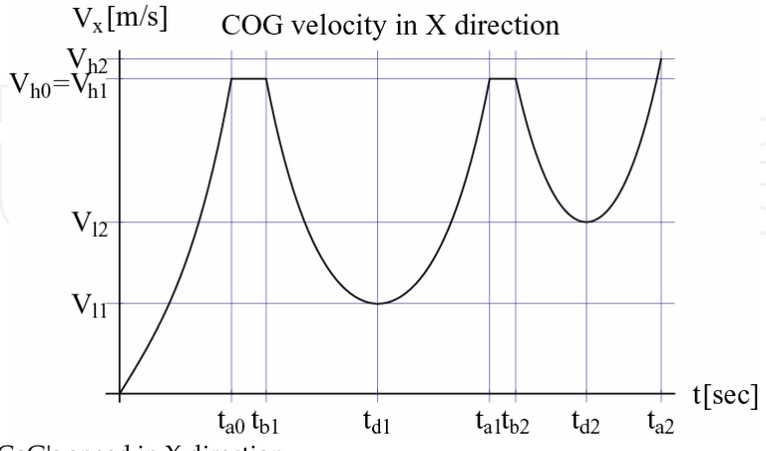

Figure 15. CoG's speed in X direction

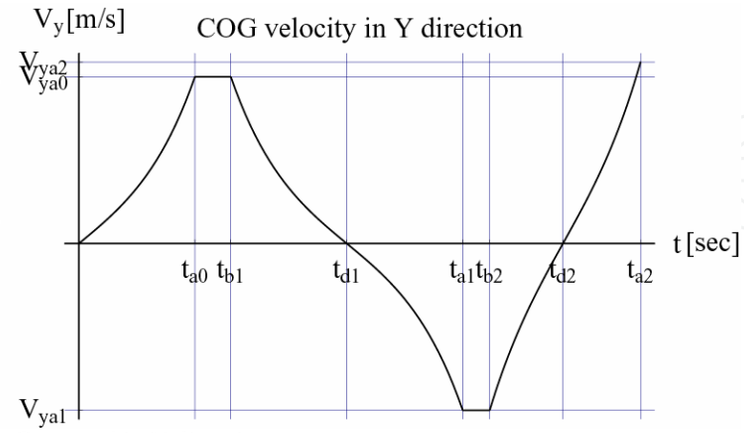

Figure 16. CoG's speed in Y direction

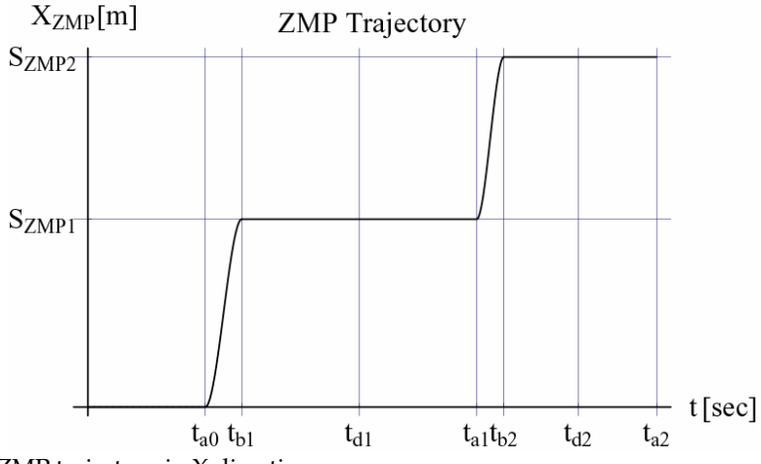

Figure 17. ZMP trajectory in X direction

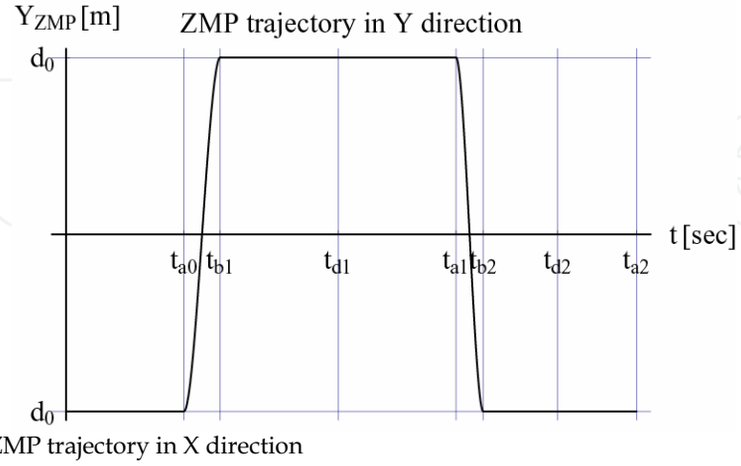

Figure 18. ZMP trajectory in X direction

S_{a0}	S_{b1}	S_{d1}	S_{a1}	S_{b2}	S_{d2}	S_{a2}	S_{ZMP1}	S_{ZMP2}	X_{s0}	d_0	Z_0
0.35	0.20	0.32	0.32	0.15	0.28	0.31	0.87	1.62	0.10	0.09	0.50
t_{a0}	t_{b1}	t_{d1}	t_{a1}	t_{b2}	t_{d2}	t_{a2}	V_{h0}	V_{l1}	V_{h1}	V_{l2}	V_{h2}
0.43	0.13	0.43	0.43	0.10	0.27	0.29	1.48	0.42	1.48	0.81	1.58
d_0	e_{s1}	e_{s2}	e_{s3}	e_{s4}	e_{s5}	e_{s6}	e_{s7}	e_{s8}	V_{ya0}	V_{ya1}	V_{ya2}
0.09	0.07	0.02	0.02	0.07	0.02	0.01	0.046	0.005	0.30	0.30	0.32

Table 1. Motion Parameters for ZMP fixed case

8. References

Hirai, K; Hirose, M.; Haikawa, Y.; & Takenaka, T. (1998), The Development of Honda Humanoid Robot, *Proceedings of the IEEE International Conference on Robotics and Automation,* pp.1321-1326, Leuven, Belgium, 1998.

Takanishi, Ishida, Yamazaki, kato (1985), Realization of Dynamic Walking on Biped Locomotion Robot WL-10RD, *Journal of Robotic Society of Japan*, vol. 3, No. 4, pp. 67-78, 1985. In Japanese.

Ogura, Y.; Aikawa, H.; Lim, H.; & Takanishi, A (2004). Development of a Human-like Walking Robot Having Two 7-DOF Legs and a 2 DOF Waist, *Proceedings of the IEEE International Conference on Robotics and Automation*, pp.134-139, New Orleans, LA, USA, 2004.

Kaneko, K.; Kanehiro, F.; Kajita, S. & et al (2004). Humanoid Robot HRP-2, *Proceedings of the IEEE International Conference on Robotics and Automation*, pp. 1083-1090, New Orleans, LA, USA, 2004.

Nakasaka, K.; & et al (2004). Integrated Motion Control for Walking, Jumping and Running on a Small Bipedal Entertainment Robot, *Proceedings of the IEEE International Conference on Robotics and Automation*, pp.3189-3194, New Orleans, LA, USA, 2004.

Löffler, K.; Gienger, M.; & Pfeiffer, F (2003). Sensor and Control Design of a Dynamically Stable Biped Robot, *Proceedings of the IEEE International Conference on Robotics and Automation*, pp.484-490, Taipei, Taiwan, 2003.

Lohmeier, S.; Löffler, K.; Gienger, M.; Ulbrich, H.; & Pfeiffer, F (2004). Computer System and Control of Biped "Johnnie", *Proceedings of the IEEE International Conference on Robotics and Automation*, pp.4222-4227, New Orleans, LA, USA, 2004.

Vukobratovich, M.; Borovac, B.; Surla, D.; & Stokic, D (1990). Biped Locomotion, Dynamics, Stability, Control and Application, Springer Verlag, 1990.

Goswami, A (1999). Postural Stability of Biped Robots and the FootRotation Indicator (FRI) Point, *International Journal of Robotics Research*, vol.19, no. 6, pp.523-533, 1999.

Kakami, S.; Nishiwaki, K.; Kitakawa, T. & et al (2000). A Fast Generation Method of a Dynamically Stable Humanoid Robot Trajectory with Enhanced ZMP Constraint, *Proceedings of the 2000 IEEE International Conference on Humanoid Robots*, CD-ROM, 2000.

Kajita, S. & Kobayashi, A (1987). Dynamic Walk Control of a Biped Robot with Potential Energy Conserving Orbit, *Transactions of the Society of Instrument and Control Engineers*, vol.23, no.3, pp.281-287, 1987, in Japanese.

Kajita, S. & et al (2002). A Real time Pattern Generator for Biped Walking, *Proceedings of the IEEE International Conference on Robotics and Automation*, Arlington VA (Washington DC), USA, pp.31-37, 2002.

Kajita, S.; & et al (2003). Biped Walking Pattern Generation by Using Preview Control of Zero-Moment Point, *Proceedings of the IEEE/RSJ International Conference on Intelligent Robots and Systems*, pp.1620-1626, Las Vegas, Nevada, USA, October 2003.

Zhu, C.; Okamura, M.; Kawamura, A.; & Tomizawa, Y (2004). Experimental approach for high speed walking of Biped Robot MARI-1, *Proceedings of the 9th International Workshop on Advanced Motion Control*, pp.427-432, 2004.

Zhu, C.; Kawamura, A (2003). Walking Principle Analysis for Biped Robot with ZMP Concept, Friction Constraint, and Inverted Pendulum Model, *Proceedings of the IEEE/RSJ International Conference on Intelligent Robots and Systems*, pp. 364-369, Las Vegas, Nevada, USA, October 2003.

Zhu, C.; Tomizawa, Y.; Luo, X.; & Kawamura, A (2004). Biped Walking with Variable ZMP, Frictional Constraint, and Inverted Pendulum Model, *Proceedings of The 2004 IEEE International Conference on Robotics and Biomimetics (ROBIO2004)*, CD-ROM, Shenyang, China. 2004.

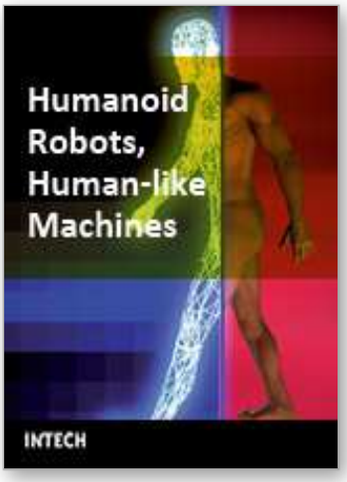

Humanoid Robots, Human-like Machines

Edited by Matthias Hackel

ISBN 978-3-902613-07-3

Hard cover, 642 pages

Publisher I-Tech Education and Publishing

Published online 01, June, 2007

Published in print edition June, 2007

In this book the variety of humanoid robotic research can be obtained. This book is divided in four parts: Hardware Development: Components and Systems, Biped Motion: Walking, Running and Self-orientation, Sensing the Environment: Acquisition, Data Processing and Control and Mind Organisation: Learning and Interaction. The first part of the book deals with remarkable hardware developments, whereby complete humanoid robotic systems are as well described as partial solutions. In the second part diverse results around the biped motion of humanoid robots are presented. The autonomous, efficient and adaptive two-legged walking is one of the main challenge in humanoid robotics. The two-legged walking will enable humanoid robots to enter our environment without rearrangement. Developments in the field of visual sensors, data acquisition, processing and control are to be observed in third part of the book. In the fourth part some "mind building" and communication technologies are presented.

InTech Europe
University Campus STeP Ri
Slavka Krautzeka 83/A
51000 Rijeka, Croatia
Phone: +385 (51) 770 447
Fax: +385 (51) 686 166
www.intechopen.com

InTech China
Unit 405, Office Block, Hotel Equatorial Shanghai
No.65, Yan An Road (West), Shanghai, 200040, China
中国上海市延安西路65号上海国际贵都大饭店办公楼405单元
Phone: +86-21-62489820
Fax: +86-21-62489821

IntechOpen